ORIGINAL SCIENTIFIC PAPER

CROATICA CHEMICA ACTA

Croat. Chem. Acta **2026**, *99*(1)
Published online: May 19, 2026
DOI: 10.5562/cca4225

HKD 1926

Halogen Bonding Induced Morphotropic Step in a Series of (Lead(II) Halogenide)–3-Halopyridine Complexes

Lucija Marić, Nikola Bedeković, Mladen Borovina, Vladimir Stilinović*

Department of Chemistry, University of Zagreb, Faculty of Science, Horvatovac 102a, 10000, Zagreb, Croatia

* Corresponding author's e-mail address: vstilinovic@chem.pmf.hr

RECEIVED: November 06, 2025 ✶ REVISED: January 22, 2026 ✶ ACCEPTED: January 23, 2026

PROCEEDING OF THE SOLUTIONS IN CHEMISTRY 2024, 11–15 NOVEMBER 2024, SVETI MARTIN NA MURI, CROATIA

Abstract: A series of nine (lead(II) halogenide)–bis(3-halopyridine) complexes (halogen = Cl, Br I) have been prepared and studied by diffraction methods. For six of them their crystal and molecular structures were determined by single crystal diffraction. The compounds were found to crystallise as two structural types – the majority (8) constitute an isostructural monoclinic ($P2_1/n$) series of with unit cell parameters 4.14 Å < a < 4.47 Å; 15.19 Å < b < 16.15 Å; 11.37 Å < c < 11.76 Å; 92.1° < β < 94.1°, while one ($PbCl_2(3Ipy)_2$) was triclinic (P–1) with unit cell volume being approximately half of that of the monoclinic series. All the compounds were found to comprise $[PbX_2(3X'py)_2]_n$ chains with pairs of halogenide ions bridging between lead ions, which are overall coordinated by four coplanar halogenide ions and a pair of pyridine ligands in an octahedral coordination. The difference between the two structural types lies in different packing of the chains, affording different halogen bonding patterns. In all structures the halogen substituents on the pyridine ligands act as halogen bond donors and halogenide anions as acceptors. However, in the monoclinic series each chain interconnects with four neighbours, while in the triclinic with only two, also allowing for a closer approach of the donor and the acceptor atoms. Computational study of molecular electrostatic potential on chain fragments has shown that the triclinic structure is favoured in cases when the halogen bond donor with the most positive σ-hole (iodopyridine), and the best acceptors with the most negative MEP (chloride and bromide) are present.

Keywords: isostructurality, halogen bonding, lead complex halogenide anion, halogenopyridine ligand.

INTRODUCTION

THE term morphotropism (or morphotropy (Morphotropie)) was originally introduced into crystallography by P. H. von Groth in 1870 to denote the effect a small change of chemical composition (such as substitution of one atom by another atom or a functional group) will affect the morphology of the crystals of the corresponding substances.[1] In his seminal 1955 Organic crystallochemistry[2] A. I. Kitaigorodsky introduced the term morphotropic step in order to denote occurrences of considerable change in crystal structure upon a small change of the molecular structure (such as replacing one halogen or chalcogen atom in a molecule with its neighbour in the group) as opposed to isomorphism, when the crystal structure is retained. A detailed analysis of numerous instances of such morphotropic steps occurring in series of crystal structures of molecular solids by A. Kálmán, has shown that the abrupt change of the structure occurs through a non-crystallographic rotation of their basic (hydrogen-bonded) motifs, such as dimers, helices, ribbons etc., whereupon the basic motif is preserved.[3–6]

A group of solids of particular interest for study isomorphism and morphotropism are halogen-bonded (XB) materials.[7–15] On the one hand, replacement of one halogen with another is likely to lead to isomorphous crystals, while on the other morphotropic step is likely to be directly caused by the change of the halogen bond energy (providing the interchanged halogen atom acts as a halogen bond donor). Particularly interesting are the cases where both the XB donor and acceptor atoms are halogens, and can thus be varied in a series of compounds. Thus it has been

demonstrated that in 3-halogenopyridinium tetrahalogenometalates the structure type is dependent on both the hydrogen and the halogen bond strength.[16] Similarly, it has been shown that the proclivity toward formation of isomorphous structures among halogenopyridinium halogenides (halogen = Cl, Br, I) depends on position of the halogen on the pyridine ring.[17–20]

We have recently demonstrated that in a series of 14 *N*-(4-halobenzyl)-3-halopyridinium halogenides only two structural types exist,[21] with the morphotropic step being induced by halogen bond. The donor-acceptor combinations yielding stronger halogen bonds forming one isostructural series, and those yielding weaker bonds the other, as well as that cocrystallization of these *N*-(4-halobenzyl)-3-halopyridinium halogenides with a neutral halogen bond donor leads to a large increase of morphotropic steps in the series of cocrystals.[22] In the present study, we have endeavoured to study the effect of halogen bond on morphotropism of coordination polymers in a series of lead(II) halogenide complexes with 3-halopyridines (halogen = Cl, Br, I).[23]

EXPERIMENTAL PROCEDURE

General Synthetic Procedure for Synthesis of $[PbX_2(3X'py)_2]_n$

The lead(II) halogenide salt is added to water and the mixture is heated under reflux conditions until the salt dissolves. In case trace amounts of the starting salt remain undissolved they are removed via filtration and 1 mL of water is added to the filtrate which is heated again until a clear solution is obtained. The lead salt solution is removed from the heater and an ethanol solution of 3-halopyridine is added to it. Crystals of products form upon cooling of the reaction mixture. Details for specific compounds can be found in ESI.

Powder X-ray Diffraction Experiments (PXRD)

PXRD experiments were performed on a Panalytical Empyrean diffractometer equipped with CuKα1 (λ = 1.54056 Å) radiation source at 40 mA and 45 kV and PIXcel3D detector in reflection mode. The angular range was from 4 to 40° (2Θ) with steps of 0.026°, and the measuring time was 0.13 s per step. Data collection and analysis was performed using the program package Data Viewer.[24]

Single crystal X-ray Diffraction Experiments (SCXRD)

The crystal and molecular structures of the prepared cocrystals were determined by single crystal X-ray diffraction. Diffraction measurements were made on Rigaku Synergy XtaLAB X-ray diffractometer with graphite-monochromated MoKα (λ = 0.71073Å) radiation. The data sets were collected using the ω scan mode over the 2Θ range up to 64°. Programs CrysAlis CCD, CrysAlis RED and CrysAlisPro were employed for data collection, cell refinement, and data reduction.[25–26] Absorption correction was performed using the multi-scan method. The structures were solved by direct methods and refined using the SHELXS, SHELXT, and SHELXL programs, respectively.[27–28]

The structural refinement was performed on F2 using all data. Hydrogen atoms were placed in calculated positions and treated as riding on their parent atoms. All calculations were performed using the WINGX crystallographic suite of programs.[29] The molecular structures of compounds and their molecular packing projections were prepared by Mercury.[30] Some of the samples have shown signs of degradation even under low (170 K) temperature. This was particularly pronounced in $(PbCl_2(3Clpy)_2$, which could not be measured at all, and this was a probable contributing factor for the rather low data quality ($PbBr_2(3Clpy)_2$, $PbBr_2(3Brpy)_2$, $PbBr_2(3Ipy)_2$, and $PbCl_2(3Brpy)_2$). This has an unfortunate consequence of rendering detailed discussion of the corresponding structures unjustified and the structural description of the monoclinic series is based on $PbI_2(3Ipy)_2$) which formed the most stable crystals, and therefore yielded the best structural data (with R = 1.41 %). Crystallographic information files are available from the Cambridge Crystallographic Data Center (CCDC) upon request (http://www.ccdc.cam.ac.uk, CCDC deposition numbers 2500572-2500577).

Computational Details

All calculations were performed using Gaussian 16 software package.[31] Single point calculations on polymer fragments generated in Mercury[30] were performed using B3LYP/def2-TZVP level of theory,[32–33] with ultrafine integration grid (99 radial shells and 590 points per shell). Figures of molecular electrostatic potential mapped to the isodensity curves of polymer fragments were prepared using GaussView.[34]

RESULTS AND DISCUSSION

A systematic screening of complexes was performed by crystallisation from solution. In all nine combinations the appearance of the product was detected. The powder diffraction patterns of the products (Figure 1) also show that 8 products ($PbCl_2(3Clpy)_2$, $PbCl_2(3Brpy)_2$, $PbBr_2(3Clpy)_2$, $PbBr_2(3Brpy)_2$, $PbI_2(3Clpy)_2$, $PbI_2(3Brpy)_2$, $PbBr_2(3Ipy)_2$ and $PbI_2(3Ipy)_2$) are apparently isostructural, as the positions of the diffraction maxima in their corresponding diffraction patterns are almost identical, and $PbCl_2(3Ipy)_2$ has evidently a different diffraction pattern, indicating a different structure.

Out of the 9 compounds in the series, six were also obtained as single crystals, albeit four of them ($PbBr_2(3Clpy)_2$, $PbBr_2(3Brpy)_2$, $PbBr_2(3Ipy)_2$, and $PbCl_2(3Brpy)_2$) yielded crystals of rather poor quality, resulting in poor quality of diffraction data. The data quality however was sufficient to prove the presumed existence of two distinct structural types. The measured single crystals of $PbCl_2(3Brpy)_2$, $PbBr_2(3Clpy)_2$, $PbBr_2(3Brpy)_2$, $PbBr_2(3Brpy)_2$, and $PbI_2(3Ipy)_2$ were found to be monoclinic ($P2_1/n$) with almost identical unit cell parameters (4.14 Å < a < 4.47 Å; 15.19 Å < b < 16.15 Å; 11.37 Å < c < 11.76 Å; 92.1° < β < 94.1°). The unit cell volume, as well as the lattice parameters a, b and c, increase monotonously with the increase of the halogen atoms present in the system, with the a parameter being primarily dependent on the halogenide anion, and b and c depending both on the halogenide anion and the halogen substituent on the pyridine ring (Figure 2). $PbCl_2(3Ipy)_2$ on the other hand was found to be triclinic (P–1), the unit cell volume being approximately half of that of the monoclinic series (380.77(6) Å^3), but with the a parameter (4.1872(3) Å) very similar to that of the monoclinic $PbCl_2(3Brpy)_2$ (4.1496(3) Å).

All the crystal structures comprise polymeric chains with pairs of halogenide anions bridging between neighbouring lead cations (Figure 3). The lead cation is in the centre of a distorted octahedron comprising four coplanar halogenide anions, and two pyridine nitrogen atoms positioned equidistantly above and below the mean plane of the $(PbX_2)_n$ chain. The halogenide anions form slightly distorted squares with one pair of Pb–X somewhat longer (by ca 0.01–0.03 Å) than the other, and the X1–Pb–X2 coordination angles generally in the range 90–93°. The Pb–X bond length follow the differences in the radii of the halogens: Pb–Cl bonds are expectedly the shortest (2.85–2.89 Å), followed by Pb–Br bonds (2.99–3.04 Å), with Pb–I bonds being the longest (ca 3.20 Å). The Pb–N bond lengths seem to be mostly independent both on the halogenide bridging the lead atoms and the halogen substituent on the pyridine ring being always in the 2.65–2.86 Å range. Also, there does not seem to be any considerable effect of the pyridine substituent on the coordination geometry of the lead(II) cation (Table 1). The planes of the pyridine rings are at approximately right angles (ca 83-86° in the monoclinic structures, and 89.4° in $PbCl_2(3Ipy)_2$) to the mean plane of the $(PbX_2)_n$ chain. In both structural types the chains extend along the crystallographic a axis, so that the a parameter corresponds to the in-chain distance between the lead atoms (Figure 2b). This explains both the dependence of the a parameter on the halogenide anion – as the in-chain distance between lead atoms is primarily dependent on the radii of the bridging halogenide anions – and the similarity of respective a parameters in $PbCl_2(3Ipy)_2$ and $PbCl_2(3Brpy)_2$, since in both cases the in-chain distance between lead atoms is determined by the bridging chloride ions.

While the configuration of the $[PbX_2(3X'py)_2]n$ chains in the two structural types is almost identical, the structures differ in their orientation and assembly in space. In the triclinic $PbCl_2(3Ipy)_2$ all the chains have the same orientation and are related by simple lattice translations, whereas in the monoclinic series the chains alternate in two

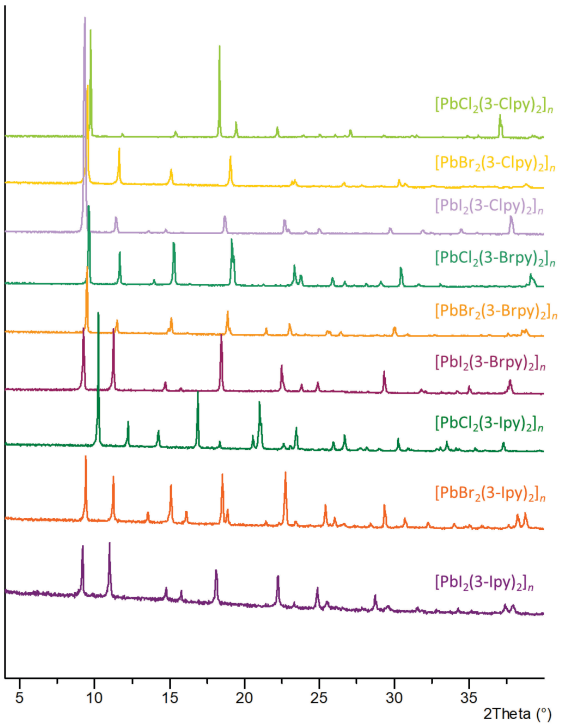

Figure 1. Powder diffraction patterns (CuKα1 (λ = 1.54056 Å) radiation) of the products obtained by crystallisation of lead(II) halogenides with 3-halopyridines.

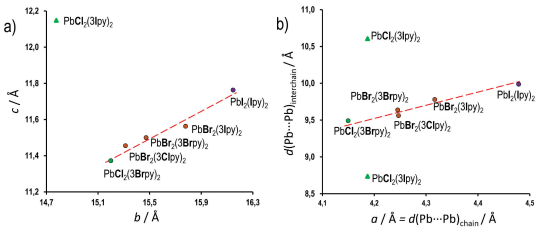

Figure 2. The trends in the change of the main features of the $PbX_2(3X'py)_2$ structures (both the monoclinic series (black bordered circles) and the triclinic $PbCl_2(3Ipy)_2$ (thick green border)) with changing the halogenides (X and X'): a) The b and c unit cell parameters (for $PbCl_2(3Ipy)_2$ the b' and c' supercell parameters are shown, see Figure 4 below for definition); b) The distances between lead atoms – in-chain distance (identical to the a unit cell parameter) and interchain distance.

orientations related by the crystallographic glide planes of the space group. The two structural types are closely related: the unit cell of the monoclinic series corresponds to a 'base-centered' supercell of double volume of the triclinic structure (Figure 4), with supercell parameters a = 4.187 Å; b' = 14.777 Å; c' = 12,619 Å; β = 101.2° (Figure 1). The morphotropic step transforming the triclinic into the monoclinic structural type can therefore be seen as rotation of every alternate chain about a twofold axis parallel to the b' of the triclinic supercell.

This rotation is related to a considerable difference in the halogen-bonded contacts between the chains. In both types of the structures each halogen atom of the halopyridine ligands acts as a donor of a halogen bond to a bridging halogenide, and each bridging halogenide is an acceptor of a halogen bond (Table 2). In $PbCl_2(3Ipy)_2$, each chain is halogen-bonded to two neighbours along the b axis, forming a centrosymmetric halogen bond motif where the same chain acts both as a halogen donor and the halogen acceptor to its two neighbours. In the monoclinic series, however, the alternating orientation of the chains leads to a 3D interconnected structure where a coordinative chain acts as a halogen bond donor to two closest neighbours and an acceptor to other two. As the result, all the inter-chain distances in the crystals of the monoclinic series are identical and increase regularly with the size of the halogen atoms in contact. In the triclinic structure however, there are two distinct types of interchain contacts, reflected in two different interchain distances – along the b axis the halogen bonded chains are considerably closer to one another than those in the monoclinic series, while along the c axis where only weak interactions are present, the interchain distances are considerably longer (Figure 2b).

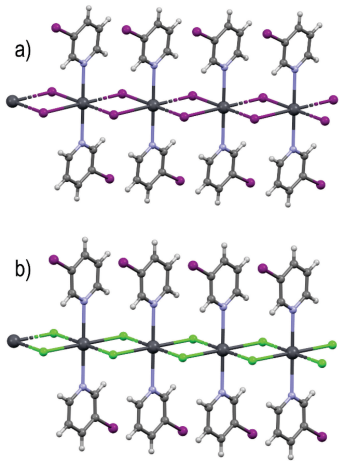

Figure 3. Fragments of the $[PbX_2(3X'py)_2]_n$ chains in crystal structures of a) $PbI_2(3Ipy)_2$ (a representative of the monoclinic isostructural series) and b) (triclinic) $PbCl_2(3Ipy)_2$. Chains are propagated in the direction of the crystallographic a axis.

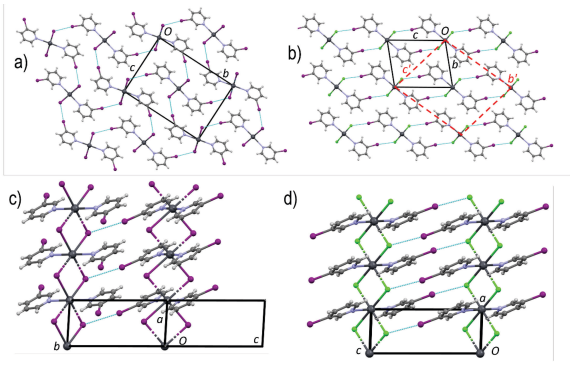

Figure 4. Packing of $[PbX_2(3X'py)_2]_n$ chains and halogen bonds between them in: a), c) $PbI_2(3Ipy)_2$ (a representative of the monoclinic isostructural series) and b), d) (the triclinic) $PbCl_2(3Ipy)_2$; a) and b) a view along the direction of the chains (the crystallographic a axis), with the construction of a supercell in b) which interconnects the triclinic structure of $PbCl_2(3Ipy)_2$ with those of the monoclinic series; c) and d) an oblique view to the direction of the chains (corresponding to <011> direction in the monoclinic series (c), and the c direction in the triclinic structure (d)) highlighting the difference in the halogen bonding pattern between neighbouring chains due to different orientation of the 3Ipy rings

Table 1. Coordination geometries around the Pb atom in the $PbX_2(3X'py)_2$ structures

Complex	d(Pb–X1)/Å	d(Pb–X2)/Å	d(Pb–N)/Å	φ(X1–Pb–X2)/°	φ(X1–Pb–N)/°	φ(X2–Pb–N)/°
$PbCl_2(3Brpy)_2$	2.850(6)	2.884(7)	2.70(2)	92.7(2)	90.9(5)	91.3(5)
$PbCl_2(3Ipy)_2$	2.859(6)	2.889(6)	2.654(16)	93.52(16)	90.8(4)	90.9(4)
$PbBr_2(3Clpy)_2$	2.9896(9)	3.0062(11)	2.683(10)	90.19(3)	90.9(2)	91.6(2)
$PbBr_2(3Brpy)_2$	2.9875(14	3.0085(15)	2.665(12)	90.14(4)	90.6(3)	92.0(3)
$PbBr_2(3Ipy)_2$	3.0037(8)	3.0343(9)	2.671(7)	91.27(2)	90.93(17)	94.05(16)
$PbI_2(3Ipy)_2$	3.19953(17)	3.2093(2)	2.686(2)	88.663(5)	90.82(6)	93.51(6)

Table 2. Halogen bond parameters in the $PbX_2(3X'py)_2$ structures

Complex	Structure type[a]	XB donor atom	XB acceptor atom	d(XB) / Å	$d(XB)_{rel}$[b]	φ(XB) / °
$PbCl_2(3Brpy)_2$	M	Br	Cl	3.434	0.9539	171.19
$PbCl_2(3Ipy)_2$	T	I	Cl	3.391	0.9091	171.02
$PbBr_2(3Clpy)_2$	M	Cl	Br	3.561	0.9892	173.36
$PbBr_2(3Brpy)_2$	M	Br	Br	3.539	0.9565	171.53
$PbBr_2(3Ipy)_2$	M	I	Br	3.591	0.9376	170.72
$PbI_2(3Ipy)_2$	M	I	I	3.750	0.9470	171.90

[a] Monoclinic(M) or Triclinic (T);
[b] d(XB) / (r_{vdW}(donor)+ r_{vdW}(acceptor))

The fact that the change from the monoclinic to the triclinic structure occurs when the constituents comprise the best halogen bond donor (iodopyridine) and the best acceptor (chloride) is a strong indication that the underlying cause of the change of structure is increased halogen bond strength. This is also supported by the observation that in some crystallisation experiments $PbBr_2(3Ipy)_2$ (comprising iodopyridine as XB donor and the second-best bromide as the acceptor) was found to form a mixture of two phases (see Figures S11 and S12 in the ESI), one of which was unequivocally identified by single crystal X-ray diffraction as the monoclinic phase, and the other characterised by a diffraction maxima at 2ϑ = 10.06°, 16.62° and 20.80° which closely correspond to the equivalent diffraction maxima of the triclinic $PbCl_2(3Ipy)_2$ (10.32°, 16.91° and 21.05°), implying that in some instances $PbBr_2(3Ipy)_2$ has also produced a triclinic polymorph, isostructural with $PbCl_2(3Ipy)_2$.

To confirm the expected potential of coordinated halopyridines as halogen bond (XB) donors, a DFT single-point computational study of chain fragments was conducted and the MEP values of the σ-holes on the central coordinated halopyridine molecule were extracted (Figure 5). As anticipated, the lowest MEP values were found on the σ-holes of the chlorine atoms of the coordinated 3Clpy molecules (average MEP = 64 kJ mol^{-1}), followed by the bromine atoms of 3Brpy (average MEP = 84 kJ mol^{-1}), and the highest values were observed on the iodine atoms of 3Ipy (average MEP = 115 kJ mol^{-1}). Generally, for the same halopyridine molecule, the MEP value in the σ-hole is highest when it is coordinated to the $(PbCl_2)_n$ fragment, slightly lower for $(PbBr_2)_n$, and lowest for $(PbI_2)_n$. Therefore, the best halogen bond donor is the 3Ipy molecule in the $PbCl_2(3Ipy)_2$ (MEP = 120 kJ mol^{-1}), while the weakest is 3Clpy in $PbI_2(3Clpy)_2$ (MEP = 61 kJ mol^{-1}).

Similar calculations were performed to rank bridging halogenide anions as halogen bond acceptors. For this purpose, hexamer fragments of $PbX_2(py)_2$ were generated, and the most negative MEP values of the central bridging halogenide were extracted (Figure 6). As a result, chloride emerged as the best acceptor site (MEP = −168 kJ mol^{-1}), followed by bromide (MEP = −141 kJ mol^{-1}) and iodide (MEP = −112 kJ mol^{-1}).

The halogen bond parameters listed in Table 1 show that the I···Cl halogen bond in $PbCl_2(3Ipy)_2$ is the shortest halogen bonding contact in the entire series of structures, with relative length being ca 91 % of the sum of the van der Waals radii of the corresponding atoms. It is ca 0.04 Å shorter than the Br···Cl halogen bond in (monoclinic) $PbCl_2(3Brpy)_2$ – in spite of larger van der Waals radius of iodine. For comparison, in the monoclinic series the halogen bonds with iodine donors (in $PbBr_2(3Ipy)_2$ and $PbI_2(3Ipy)_2$) both have relative lengths ca 93–94 % of the sum of the van der Waals radii of the corresponding atoms (this raising to 95–96 % for the two bromine donors and ca 99 % in the only structure with the chlorine donor). Also, within the (monoclinic) $PbBr_2$ derivatives, the I···Br halogen

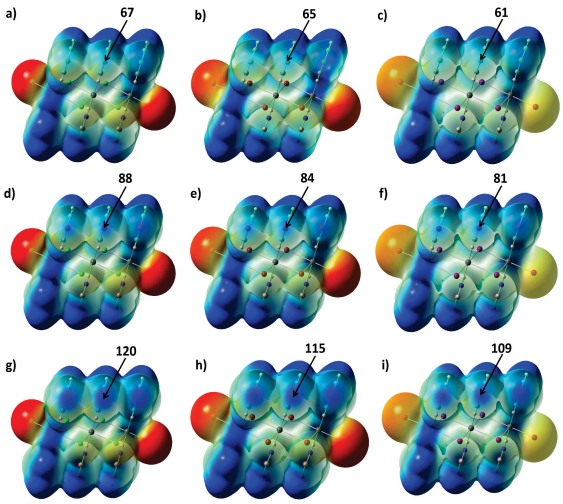

Figure 5. Molecular electrostatic potential plotted on isodensity surface (0.001 a.u.) of a) $[PbCl_2(3Clpy)_2]_3$; b) $[PbBr_2(3Clpy)_2]_3$; c) $[PbI_2(3Clpy)_2]_3$; d) $[PbCl_2(3Brpy)_2]_3$; e) $[PbBr_2(3Brpy)_2]_3$; f) $[PbI_2(3Brpy)_2]_3$; g) $[PbCl_2(3Ipy)_2]_3$; h) $[PbBr_2(3Ipy)_2]_3$; i) $[PbI_2(3Ipy)_2]_3$.

bond is longer than the Br···Br bond, reflecting the difference of the van der Waals radii of bromine and iodine. All of this clearly indicates that the assembly of the $[PbX_2(3X'py)_2]_n$ chains in the triclinic type of stuctures (represented by $PbCl_2(3Ipy)_2$) allows for closer approach of the donor atom to the acceptor and therefore stronger halogen bond. As the importance of this increases with the positive potential of the halogen bond donor σ-hole and the negative potential on the acceptor atom, the morphotropic step – i.e. the change of the structural type from the monoclinic to the triclinic – occurs only in the cases which combine the best donor (iodine), with best acceptors (coordinated chloride and, to an extent, bromide).

CONCLUSION

The studied series of coordination polymers provides an interesting case of halogen bond induced morphotropism. When only weaker halogen bond donors (chloro- and bromopyridine, with σ-hole MEP below 88 kJ mol^{-1}), or poorer acceptor (bridging iodide, with average MEP_{min} −112 kJ mol^{-1}) are present only the monoclinic structure type is observed. However, when the strongest halogen bond donor of the series (iodopyridine, average MEP_{max} 115 kJ mol^{-1}) and the best acceptor (chloride, MEP_{min} = −168 kJ mol^{-1}) are present, the coordination polymeric chains rotate, so that they allow for a closer contact between the donor and the acceptor, leading to appearance of the triclinic phase. The fact that the second-best acceptor (bromide), when combined with iodopyridine apparently can yield both phases indicated that the halogen bond energy between iodopyridine and coordinated bromine is close to the 'tipping point' between the two structural types. This would make a direct comparison of the structures (and packing energies) of the two polymorphs of $PbBr_2(3Ipy)_2$ very interesting indeed. While we were not able to procure suitable single crystals (or pure samples) as a part of this study, further investigations in this direction are under way.

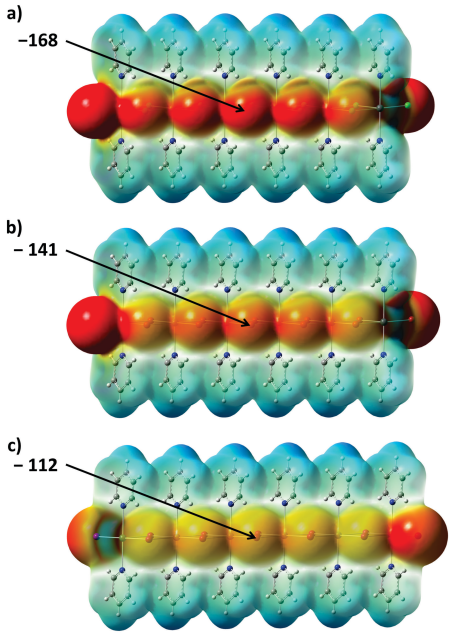

Figure 6. Molecular electrostatic potential plotted on isodensity surface (0.001 a.u.) of a) $[PbCl_2(py)_2]_6$; b) $[PbBr_2(py)_2]_6$; c) $[PbI_2(py)_2]_6$.

Supplementary Information. Supporting information to the paper is attached to the electronic version of the article at: https://doi.org/10.5562/cca4225.

PDF files with attached documents are best viewed with Adobe Acrobat Reader which is free and can be downloaded from Adobe's web site.

REFERENCES

[1] P. Groth, *Ann. der Phys.* **1870**, *217*, 31–43. https://doi.org/10.1002/andp.18702170904

[2] A. I. Kitaigorodsky, Organicheskaya Kristallochimia; Izdatelstvo akademii nauk SSSR: Moscow, **1955**.

[3] A. Kálmán, *Acta Crystallogr., Sect. B.* **2005**, *B61*, 536–547. https://doi.org/10.1107/S0108768105023189

[4] A. Kálmán, L. Párkányi, G. Argay, *Acta Crystallogr., Sect. B.* **1993**, *B49*, 1039–1049. https://doi.org/10.1107/S010876819300610X

[5] A. Kálmán, G. Argay, L. Fábián, G. Bernáth, F. Fülöp, *Acta Crystallogr., Sect. B.* **2001**, *B57*, 539–550. https://doi.org/10.1107/S0108768101006723

[6] A. Kálmán, L. Fábián, G. Argay, G. Bernáth, Z. Gyarmati, *Acta Crystallogr., Sect. B.* **2002,** *B58*, 855–863. https://doi.org/10.1107/S0108768102009631

[7] D. Cinčić, T. Friščić, W. Jones, *Chem. Mater.* **2008**, *20*, 6623–6626. https://doi.org/10.1021/cm800923r

[8] D. Cinčić, T. Friščić, W. Jones, *J. Am. Chem. Soc.* **2008**, *130*, 7524–7525. https://doi.org/10.1021/ja801164v

[9] D. Cinčić, T. Friščić, W. Jones, *New J. Chem.* **2008**, *3*, 1776–1781. https://doi.org/10.1039/b805816d

[10] D. Cinčić, T. Friščić, W. Jones, *Chem. Mater.* **2008** *20*, 6623–6626. https://doi.org/10.1021/cm800923r

[11] A. V. Buldakov, M. A. Kinzhalov, M. A. Kryukova, D. M. Ivanov, A. S. Novikov, A. S. Smirnov, G. L. Starova, N. A. Bokach, V. Y. Kukushkin, *Cryst. Growth Des.* **2020**, *20*, 1975–1984. https://doi.org/10.1021/acs.cgd.9b01631

[12] S. A. Adonin, M. A. Bondarenko, A. S. Novikov, M. N. Sokolov, *Crystals* **2020**, *10,* 289. https://doi.org/10.3390/cryst10040289

[13] A. Dey, G. R. Desiraju, *CrystEngComm* **2004**, *6*, 642–646. https://doi.org/10.1039/b416962j
[14] A. Abate, J. Martí-Rujas, P. Metrangolo, T. Pilati, G. Resnati, G. Terraneo, *Cryst. Growth Des.* **2011**, *11*, 4220–4226. https://doi.org/10.1021/cg200840m
[15] J. C. Bennion, L. Vogt, M. E. Tuckerman, A. J. Matzger, *Cryst. Growth Des.* **2016**, *16*, 4688–4693. https://doi.org/10.1021/acs.cgd.6b00753
[16] -G. M. Espallargas, F. Zordan, L. A. Marín, H. Adams, K. Shankland, J. De Van Streek, L. Brammer, *Chem. - A Eur. J.* **2009**, *15*, 7554–7568. https://doi.org/10.1002/chem.200900410
[17] F. F. Awwadi, R. D. Willett, K. A. Peterson, B. Twamley, *J. Phys. Chem. A* **2007**, *111*, 2319–2328. https://doi.org/10.1021/jp0660684
[18] M. Freytag, P. G. Jones, B. Ahrens, A. K. Fischer, *New J. Chem.* **1999**, *23*, 1137–1139. https://doi.org/10.1039/a906356k
[19] M. Freytag, P. G. Jones, *Zeitschrift fur Naturforsch. - Sect. B* **2001**, *56*, 889–896. https://doi.org/10.1515/znb-2001-0905
[20] L. Fotović, V. Stilinović, *CrystEngComm* **2020**, *22*, 4039–4046. https://doi.org/10.1039/d0ce00534g
[21] L. Fotović, N. Bedeković, V. Stilinović, *Cryst. Growth Des.* **2022**, *22*, 1333–1344. https://doi.org/10.1021/acs.cgd.1c01285
[22] N. Baus Topić, E. Topić, L. Fotović, V. Stilinović, *Cryst. Growth Des.* 2024, 24, 3, 1214–1226. https://doi.org/10.1021/acs.cgd.3c01189
[23] H. Miyamae, H. Toriyama, T. Abe, G. Hihara, M. Nagata *Acta Cryst.* **1984**, *C40*, 1559–1562. https://doi.org/10.1107/S0108270184008702
[24] B.V. Amelo, PANalytical The Netherlands, Data Viewer, Version 1.9a, **2018**.
[25] Oxford Diffraction, Oxford Diffraction Ltd., Xcalibur CCD system, CrysAlis CCD and CrysAlis RED software, Version 1.170, **2003**.
[26] Rigaku Oxford Diffraction, Gemini CCD system, CrysAlis Pro software, Version 171.41.93a, **2020**.
[27] G. M. Sheldrick, *Acta Cryst. A* **2008**, *64*, 112–122. https://doi.org/10.1107/S0108767307043930
[28] G. M. Sheldrick, *Acta Cryst. C* **2015**, *71*, 3–8. https://doi.org/10.1107/S2053229614024218
[29] L. J. Farrugia, *J. Appl. Cryst.* **2012**, *45*, 849–854. https://doi.org/10.1107/S0021889812029111
[30] C. F. Macrae, I. J. Bruno, J. A. Chisholm, P. R. Edgington, P. McCabe, E. Pidcock, L. Rodriguez-Monge, R. Taylor, J. v. d. Streek, P. A. Wood *J. Appl. Crystallogr*. **2008**, *41*, 466–470. https://doi.org/10.1107/S0021889807067908
[31] Gaussian 16, Revision C.01, M. J. Frisch, G. W. Trucks, H. B. Schlegel, G. E. Scuseria, M. A. Robb, J. R. Cheeseman, G. Scalmani, V. Barone, G. A. Petersson, H. Nakatsuji, X. Li, M. Caricato, A. V. Marenich, J. Bloino, B. G. Janesko, R. Gomperts, B. Mennucci, H. P. Hratchian, J. V. Ortiz, A. F. Izmaylov, J. L. Sonnenberg, D. Williams-Young, F. Ding, F. Lipparini, F. Egidi, J. Goings, B. Peng, A. Petrone, T. Henderson, D. Ranasinghe, V. G. Zakrzewski, J. Gao, N. Rega, G. Zheng, W. Liang, M. Hada, M. Ehara, K. Toyota, R. Fukuda, J. Hasegawa, M. Ishida, T. Nakajima, Y. Honda, O. Kitao, H. Nakai, T. Vreven, K. Throssell, J. A. Montgomery, Jr., J. E. Peralta, F. Ogliaro, M. J. Bearpark, J. J. Heyd, E. N. Brothers, K. N. Kudin, V. N. Staroverov, T. A. Keith, R. Kobayashi, J. Normand, K. Raghavachari, A. P. Rendell, J. C. Burant, S. S. Iyengar, J. Tomasi, M. Cossi, J. M. Millam, M. Klene, C. Adamo, R. Cammi, J. W. Ochterski, R. L. Martin, K. Morokuma, O. Farkas, J. B. Foresman, D. J. Fox Gaussian, Inc., Wallingford CT, **2016**.
[32] A. D. Becke, *J. Chem. Phys*. **1993**, *98*, 5648–5652. https://doi.org/10.1063/1.464913
[33] C. Lee, W. Yang, R. G. Parr, *Phys. Rev. B* **1988**, *37*, 785–789. https://doi.org/10.1103/PhysRevB.37.785
[34] GaussView, Version 5.1; R. Dennington, T. A. Keith, J. M. Millam, (Eds.) Semichem Inc.: Shawnee, KS, USA, **2008**.